

Comparative Study of Structure Formation, Recombination, and Matter–Radiation Equality in $f(R, L_m)$ Gravity and Λ CDM Cosmology

G. K. Goswami^{1,*} and J. P. Saini^{2,†}

¹*Department of Mathematics, Netaji Subhas University of Technology, New Delhi 110078, India*

²*Vice Chancellor, Madan Mohan Malviya University of Technology, Gorakhpur, Uttar Pradesh 273010, India*

We present a comprehensive comparative analysis of three pivotal epochs in cosmic history—structure formation, recombination, and matter–radiation equality, within the framework of $f(R, L_m)$ gravity and the standard Λ CDM cosmology. Using a nonlinear evolution equation for density perturbations, we determine the collapse redshift (z_c), showing that cosmic structures form earlier in $f(R, L_m)$ gravity due to enhanced effective gravitational coupling. Recombination is studied via the visibility function $g(z)$, peaking at $z_{\text{rec}} \approx 1092.6$ in both models, consistent with Planck 2018 data. We compute the full width at half maximum (FWHM) of $g(z)$ and find a slightly extended decoupling duration in $f(R, L_m)$. Finally, we analyze the evolution of energy densities and determine the matter–radiation equality redshift as $z_{\text{eq}} \approx 4203$ in $f(R, L_m)$ and $z_{\text{eq}} \approx 2779$ in Λ CDM, with corresponding cosmic times of approximately 67,756 and 67,232 years, respectively. These results confirm that $f(R, L_m)$ gravity retains key cosmological landmarks while introducing testable deviations from the standard paradigm.

PACS numbers: 98.80.-k, 98.80.Es, 04.50.Kd

Keywords: Modified gravity; $f(R, L_m)$ theory; cosmological perturbations; observational constraints; FLRW universe

I. INTRODUCTION

Understanding the dynamics of the early Universe remains one of the most compelling pursuits in modern cosmology. The standard cosmological model, Λ CDM, built upon General Relativity (GR) and a cosmological constant, has achieved remarkable success in explaining a broad range of observations, including the cosmic microwave background (CMB) [1], baryon acoustic oscillations [2], large-scale structure formation [3, 4], and the late-time acceleration of the Universe [5–7].

Despite its triumphs, Λ CDM faces theoretical challenges such as the fine-tuning problem associated with the cosmological constant, the absence of a fundamental explanation for dark energy, and its limited compatibility with quantum gravity frameworks. These open issues have motivated the exploration of alternative theories of gravity, including $f(R)$ gravity [8], $f(R, T)$ gravity [9], scalar-tensor theories [10], Gauss-Bonnet modifications [11], and non-minimally coupled models such as $f(R, L_m)$ gravity [12, 13].

The $f(R, L_m)$ gravity framework extends the Einstein–Hilbert action by allowing the Lagrangian to depend on both the Ricci scalar R and the matter Lagrangian L_m :

$$S = \int \left[\frac{1}{2\kappa} f(R, L_m) \right] \sqrt{-g} d^4x,$$

* gk.goswami9@gmail.com

† jps@mmmut.ac.in

where $\kappa = 8\pi G$. This curvature–matter coupling modifies the field equations, leads to non-conservation of the energy–momentum tensor, and alters both background cosmological evolution and structure formation dynamics. Several studies have investigated its implications for cosmic acceleration [12], inflation [13], and large-scale structure [14].

In the quest to understand the origin and evolution of cosmic structures, several key epochs in the early Universe play a foundational role. The *recombination era* [15–17], occurring at redshift $z \sim 1100$, marks the epoch when neutral hydrogen formed and photons decoupled from baryons, giving rise to the cosmic microwave background [18, 19]. Following recombination, the growth of small matter density perturbations led to the formation of nonlinear structures such as galaxies and clusters [20–22], a process governed by the underlying gravitational theory. Another pivotal milestone is the *matter–radiation equality* epoch [23–25], which defines the transition from radiation-dominated to matter-dominated expansion, strongly influencing the subsequent evolution of perturbations.

In this work, we examine these epochs in the context of the modified gravity framework $f(R, L_m)$, comparing their timing and characteristics with the predictions of the standard Λ CDM model. These comparisons provide crucial insights into the viability of non-minimally coupled theories in explaining early-Universe dynamics and observational features. Specifically, we investigate three key epochs in cosmic history:

1. **Structure Formation:** We analyze the nonlinear growth of matter overdensities and compute the redshift of collapse z_c .
2. **Recombination Era:** We study the visibility function and its full width at half maximum (FWHM) to determine the timing and duration of photon decoupling.
3. **Matter–Radiation Equality:** We compute the redshift z_{eq} and the cosmic time t_{eq} at which matter and radiation densities were equal.

Our results show that the $f(R, L_m)$ model can reproduce essential cosmological milestones such as recombination and matter–radiation equality while allowing for enhanced structure formation compared to Λ CDM. These findings reinforce the potential of curvature–matter coupling as a compelling extension to GR, offering testable deviations from standard cosmology.

II. THEORETICAL FRAMEWORK AND STATISTICAL RESULTS

We consider a curvature–matter coupling model defined by the Lagrangian [14]:

$$f(R, L_m) = \alpha R + L_m^\beta + \gamma,$$

where R is the Ricci scalar, L_m is the matter Lagrangian density, and α , β , and γ are model parameters. This functional form modifies the cosmic expansion history and the evolution of matter through non-minimal coupling between curvature and matter.

Assuming a spatially flat FLRW universe and a perfect fluid with barotropic equation of state $p = (1-n)\rho$, the modified Friedmann equation becomes:

$$H^2(z) = \left(\frac{\gamma}{6\alpha} + H_0^2 \right) (1+z)^{\frac{3\beta n}{2\beta-1}} - \frac{\gamma}{6\alpha}.$$

This can be recast in the standard form:

$$H(z) = H_0 \sqrt{(1 - \lambda) + \lambda(1 + z)^{3(1+w)}},$$

where the effective parameters are given by:

$$\lambda = \frac{\gamma}{6\alpha H_0^2} + 1, \quad w = \frac{\beta(n-2) + 1}{2\beta - 1}.$$

Energy Density Evolution

The corresponding matter energy density evolves according to:

$$\rho(z) = \left(\frac{\gamma + 6\alpha H^2(z)}{2\beta - 1} \right)^{1/\beta}.$$

This evolution reflects the influence of the curvature–matter interaction, deviating from the standard $(1+z)^3$ scaling.

Statistical Analysis

We perform parameter estimation using a two-step strategy. First, a chi-square minimization provides initial best-fit values. This is followed by a Bayesian Markov Chain Monte Carlo (MCMC) analysis to explore the full posterior distribution. A neural network–based regression approach is also employed to cross-validate the results.

The outcomes are visualized through corner plots of the posterior distributions, as well as error bar plots comparing theoretical predictions with observational data for the Hubble parameter and distance modulus.

Results and Discussion

The best-fit parameters for the $f(R, L_m)$ model (at 68% confidence level) are:

$$H_0 = 73.75 \pm 0.16 \text{ km s}^{-1} \text{ Mpc}^{-1}, \quad \lambda = 0.262 \pm 0.007, \quad w = -0.005 \pm 0.001.$$

For comparison, the Λ CDM model yields:

$$H_0 = 73.49 \pm 0.14 \text{ km s}^{-1} \text{ Mpc}^{-1}, \quad \Omega_m = 0.278 \pm 0.006.$$

These results suggest that both models support a relatively high Hubble constant, consistent with local measurements. However, the $f(R, L_m)$ model permits small but non-negligible deviations from standard cosmology. These are captured by the effective parameters λ and w , offering increased flexibility to describe both early- and late-time cosmic dynamics.

III. EARLY-TIME STRUCTURE FORMATION AND COLLAPSE REDSHIFT ANALYSIS IN $f(R, L_m)$ GRAVITY

As an extension of the growth rate analysis presented previously [14], we now investigate the early-time behavior of matter perturbations, focusing on identifying the redshift at which nonlinear structure formation begins in the $f(R, L_m)$ gravity model.

To this end, we analyze the evolution of the linear matter density contrast $\delta(z)$ in redshift space, within the modified gravity framework.

Perturbation Growth Equation

In redshift space, the evolution of linear matter perturbations is governed by the second-order differential equation:

$$\frac{d^2\delta}{dz^2} + \left(\frac{d\ln H}{dz} - \frac{2}{1+z} \right) \frac{d\delta}{dz} - \frac{3}{2} \frac{G_{\text{eff}}(z) \rho(z)}{H^2(z) (1+z)^2} \delta = 0, \quad (1)$$

where $H(z)$ is the Hubble parameter, $\rho(z)$ is the background matter energy density, and the effective gravitational coupling is given by

$$G_{\text{eff}}(z) = \frac{(2\beta - 1)\beta \rho^{\beta-1}}{\alpha}.$$

For numerical stability, we reformulate the equation using the logarithmic variable $u(z) = \ln \delta(z)$, leading to:

$$\frac{d^2u}{dz^2} + \left(\frac{d\ln H}{dz} - \frac{2}{1+z} \right) \frac{du}{dz} - \frac{3}{2} \frac{G_{\text{eff}}(z) \rho(z)}{H^2(z) (1+z)^2} = 0. \quad (2)$$

Model Parameters and Initial Conditions

The best-fit parameters used in this analysis are:

$$\begin{aligned} H_0 &= 73.75 \text{ km s}^{-1} \text{ Mpc}^{-1}, & \lambda &= 0.262, & w &= -0.005, \\ \alpha &= 451008, & \beta &= 1.00505, & \gamma &= -1.14081 \times 10^{-29}. \end{aligned}$$

Initial conditions are specified at redshift $z = 100$:

$$\delta(z) = \frac{1}{1+z}, \quad \frac{d\delta}{dz} = -\frac{1}{(1+z)^2}.$$

Collapse Redshift Criterion

The collapse redshift z_c is defined as the redshift at which the matter overdensity becomes nonlinear, i.e.,

$$\delta(z_c) = 1.686.$$

Solving the perturbation equation numerically, we find:

$$z_c^{f(R, L_m)} \approx 25.56,$$

indicating that structure formation commences significantly earlier in the $f(R, L_m)$ model compared to standard cosmology.

IV. COMPARISON WITH Λ CDM COSMOLOGY

To compare with the standard model, we perform a parallel analysis under the Λ CDM framework. The form of the perturbation equation remains the same, but with:

$$G_{\text{eff}} = G, \quad \rho(z) = \rho_{m,0}(1+z)^3.$$

The best-fit parameters used for Λ CDM are:

$$H_0 = 73.49 \text{ km s}^{-1} \text{ Mpc}^{-1}, \quad \Omega_m = 0.278.$$

Applying the same initial conditions at $z = 100$, we find that the perturbation does not reach the collapse threshold by $z = 0$, leading to the conclusion:

$$z_c^{\Lambda\text{CDM}} : \text{No collapse within the considered redshift range}.$$

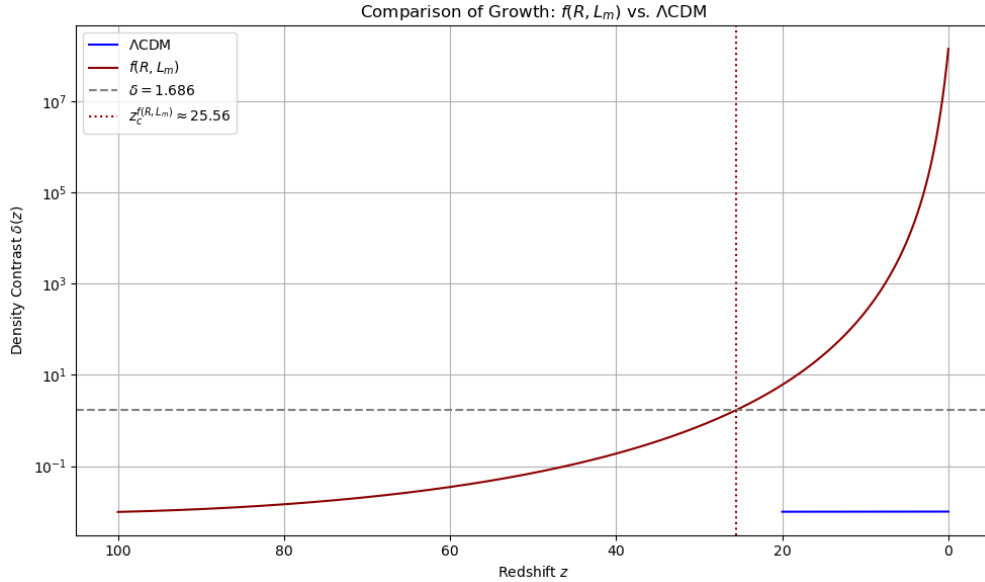


FIG. 1: Evolution of the density contrast $\delta(z)$ in $f(R, L_m)$ and Λ CDM models. The red dashed line denotes the collapse threshold $\delta = 1.686$. The $f(R, L_m)$ model predicts collapse at $z_c \approx 25.56$, whereas the Λ CDM model does not reach this value by $z = 0$.

TABLE I: Collapse Redshift Comparison

Model	Collapse Redshift z_c	Interpretation
$f(R, L_m)$	25.56	Early formation of bound structures
Λ CDM	<i>No collapse by $z = 0$</i>	Delayed growth, late-time structure formation

Discussion and Implications

The much earlier collapse in the $f(R, L_m)$ model is attributed to the enhanced effective gravitational coupling $G_{\text{eff}}(z)$ at high redshifts. This could result in observable imprints in the abundance of early galaxies, high-redshift clusters, and the reionization epoch.

Effective Collapse Threshold and Comparative Growth

To enable a fair comparison with the $f(R, L_m)$ result ($z_c \approx 25.56$), we consider reduced effective collapse thresholds in the Λ CDM model:

$$\delta_{\text{eff}} = 1.0, \quad 1.3, \quad 1.5,$$

which represent progressively significant nonlinear growth phases.

TABLE II: Effective Collapse Redshift in Λ CDM for Various Thresholds

Threshold δ_{eff}	Approximate z_c^{eff}
1.0	$z \approx 1.1$
1.3	$z \approx 0.7$
1.5	$z \approx 0.4$

Despite lowering the threshold, the growth in Λ CDM remains markedly slower than in $f(R, L_m)$. This highlights a key advantage of the modified gravity scenario in facilitating early structure formation. Upcoming observations from galaxy surveys and 21 cm cosmology may provide crucial tests to distinguish between these models.

V. RECOMBINATION ERA AND IMPLICATIONS IN $f(R, L_m)$ GRAVITY

The recombination epoch marks a pivotal phase in cosmic history, when the Universe cooled sufficiently for free electrons and protons to form neutral hydrogen. This dramatically reduced the photon scattering rate, allowing photons to decouple from matter and propagate freely—giving rise to the Cosmic Microwave Background (CMB).

Standard Scenario in Λ CDM

In the Λ CDM model, the redshift of recombination is estimated via the temperature-redshift relation:

$$T(z_{\text{rec}}) = T_0(1 + z_{\text{rec}}) \approx 3000 \text{ K}, \quad T_0 = 2.725 \text{ K},$$

yielding a rough estimate:

$$z_{\text{rec}} \approx \frac{3000}{2.725} \approx 1101.$$

More precisely, the Planck 2018 results report:

$$z_{\text{rec}}^{\Lambda\text{CDM}} \approx 1089.9 \pm 0.4.$$

Photon Decoupling in $f(R, L_m)$ Gravity

While the atomic physics governing recombination remains unchanged, the expansion rate $H(z)$ in $f(R, L_m)$ gravity deviates from ΛCDM due to the curvature–matter coupling. This modified expansion can influence the timing and duration of photon decoupling.

The differential optical depth is expressed as:

$$\frac{d\tau}{dz} = \frac{c \sigma_T n_e(z)}{(1+z) H(z)},$$

where σ_T is the Thomson scattering cross-section, and $n_e(z)$ is the free electron number density.

The visibility function, representing the probability that a photon last scattered at redshift z , is defined as:

$$g(z) = \frac{d\tau}{dz} e^{-\tau(z)}.$$

For both models, we adopt the following approximate ionization profile:

$$x_e(z) = \frac{1}{1 + e^{(z-z_{\text{rec}})/\Delta z}}, \quad n_e(z) = x_e(z) n_{b,0} (1+z)^3,$$

with $\Delta z \approx 80$ and $n_{b,0}$ denoting the present-day baryon number density.

Recombination Redshift and Duration

Using the best-fit parameters:

$$\begin{aligned} f(R, L_m): \quad & H_0 = 73.75 \text{ km s}^{-1} \text{ Mpc}^{-1}, \quad \lambda = 0.262, \quad w = -0.005, \\ \Lambda\text{CDM}: \quad & H_0 = 73.49 \text{ km s}^{-1} \text{ Mpc}^{-1}, \quad \Omega_m = 0.278, \quad \Omega_\Lambda = 1 - \Omega_m, \end{aligned}$$

we numerically compute the optical depth and visibility function $g(z)$ for both models.

TABLE III: Recombination Redshift and FWHM Comparison

Model	Recombination Redshift z_{rec}	FWHM Δz
$f(R, L_m)$	1092.6	166.2
ΛCDM	1092.6	153.3

Both models yield identical recombination redshifts, consistent with Planck observations. However, the $f(R, L_m)$ model exhibits a slightly broader full width at half maximum (FWHM), suggesting a more extended duration of photon decoupling.

Visibility Function and FWHM Analysis

The FWHM corresponds to the redshift range where $g(z) \geq \frac{1}{2}g_{\text{max}}$. In the $f(R, L_m)$ model, the visibility function remains above half its peak between:

$$z \in [1010.1, 1176.3] \Rightarrow \Delta z \approx 166.2.$$

For ΛCDM , the range is:

$$z \in [1018.9, 1172.2] \Rightarrow \Delta z \approx 153.3.$$

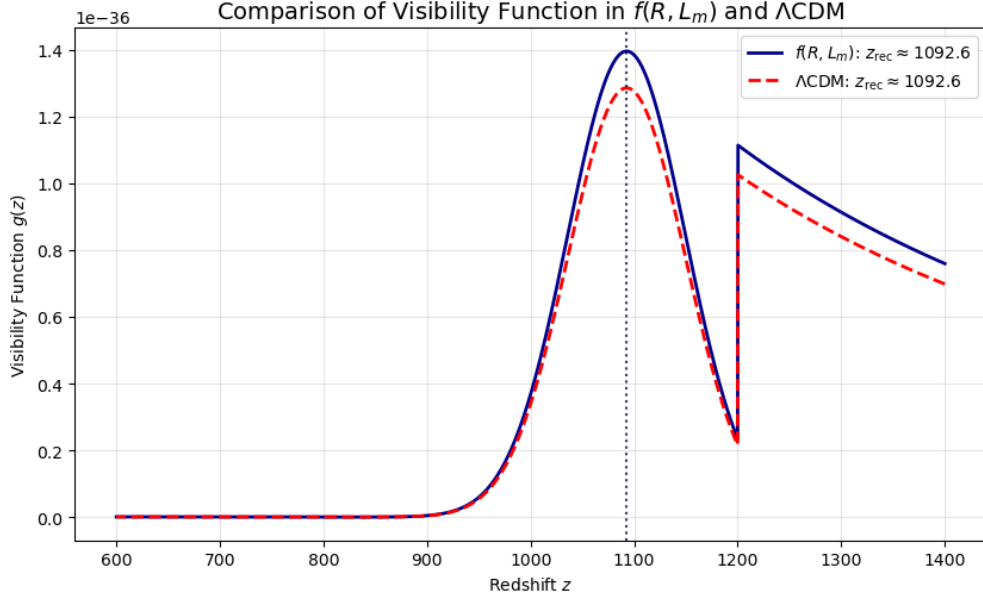


FIG. 2: Visibility function $g(z)$ for both $f(R, L_m)$ and ΛCDM models. The peaks coincide at $z_{\text{rec}} \approx 1092.6$. The shaded bands show the FWHM, which is broader in the $f(R, L_m)$ model, indicating a more extended recombination era.

Interpretation and Implications

The broader FWHM in the $f(R, L_m)$ model implies a slightly more gradual transition from opaque to transparent Universe. This extended recombination duration arises from differences in the expansion history governed by the modified gravity framework.

Although subtle, such effects may imprint on the CMB power spectrum, particularly in the damping tail and higher-order acoustic peaks. Thus, the recombination history in $f(R, L_m)$ gravity retains consistency

with observational benchmarks while offering new avenues for distinguishing modified gravity models from Λ CDM using precise CMB data.

MATTER AND RADIATION ENERGY DENSITIES AND THEIR EQUALITY IN Λ CDM AND $f(R, L_m)$ GRAVITY

In the standard cosmological model (Λ CDM), the energy–momentum tensor is covariantly conserved:

$$\nabla_\mu T^{\mu\nu} = 0.$$

For non-interacting perfect fluids, this yields the continuity equation:

$$\frac{d\rho}{dt} + 3H(\rho + p) = 0,$$

leading to the standard redshift scalings:

$$\begin{aligned}\rho_m(z) &= \rho_{m0}(1+z)^3, & (\text{dust}), \\ \rho_r(z) &= \rho_{r0}(1+z)^4, & (\text{radiation}).\end{aligned}$$

Thus, the total energy density evolves as:

$$\rho_{\text{tot}}(z) = \rho_m(z) + \rho_r(z),$$

which enters the Friedmann equation:

$$H^2(z) = H_0^2 [\Omega_m(1+z)^3 + \Omega_r(1+z)^4 + \dots].$$

In contrast, the $f(R, L_m)$ gravity model introduces a non-minimal coupling between matter and geometry, leading generally to:

$$\nabla_\mu T^{\mu\nu} \neq 0.$$

As a result, the matter energy density does not obey the standard $(1+z)^3$ scaling. However, assuming radiation is minimally coupled, its redshift dependence remains:

$$\rho_r(z) = \rho_{r0}(1+z)^4.$$

Hence, the total energy density in the $f(R, L_m)$ model becomes:

$$\rho_{\text{tot}}^{f(R, L_m)}(z) = \rho_m^{f(R, L_m)}(z) + \rho_{r0}(1+z)^4,$$

where $\rho_m^{f(R, L_m)}(z)$ is derived from the modified field equations.

Matter–Radiation Equality in $f(R, L_m)$ Gravity

In both models, the redshift of matter–radiation equality is defined by:

$$\rho_m(z_{\text{eq}}) = \rho_r(z_{\text{eq}}).$$

For radiation:

$$\rho_r(z) = \rho_{r0}(1+z)^4,$$

while for matter in $f(R, L_m)$ gravity:

$$\rho_m(z) = \left(\frac{\gamma + 6\alpha H^2(z)}{2\beta - 1} \right)^{1/\beta},$$

with:

$$H(z) = H_0 \sqrt{(1-\lambda) + \lambda(1+z)^{3(1+w)}},$$

and best-fit parameters:

$$\begin{aligned} H_0 &= 2.39007 \times 10^{-18} \text{ s}^{-1}, \quad \lambda = 0.262, \quad w = -0.005, \\ \alpha &= 451008, \quad \gamma = -1.14081 \times 10^{-29}. \end{aligned}$$

Solving $\rho_m(z_{\text{eq}}) = \rho_r(z_{\text{eq}})$ numerically, we obtain:

$$\boxed{z_{\text{eq}}^{f(R, L_m)} \approx 4203.2}.$$

The corresponding cosmic time is computed via:

$$t(z) = \int_z^\infty \frac{1}{(1+z') H(z')} dz',$$

yielding:

$$\boxed{t_{\text{eq}}^{f(R, L_m)} \approx 67,756 \text{ years}}.$$

1. Matter–Radiation Equality in Λ CDM

Using:

$$\Omega_m = 0.278, \quad \Omega_r = 0.0001,$$

the equality redshift is given by:

$$z_{\text{eq}}^{\Lambda\text{CDM}} \approx 2779.$$

With the standard ΛCDM Hubble rate:

$$H(z) = H_0 \sqrt{\Omega_m(1+z)^3 + \Omega_r(1+z)^4 + \Omega_\Lambda},$$

the integration yields:

$$t_{\text{eq}}^{\Lambda\text{CDM}} \approx 67,232 \text{ years}.$$

This earlier transition to matter domination in the $f(R, L_m)$ model is noteworthy, as it supports the earlier onset of structure formation discussed in prior sections.

TABLE IV: Matter–radiation equality in ΛCDM and $f(R, L_m)$ gravity. The higher z_{eq} in $f(R, L_m)$ implies earlier matter domination.

Model	Equality Redshift z_{eq}	Cosmic Time t_{eq} (years)
ΛCDM	2779.0	67,232
$f(R, L_m)$	4203.2	67,756

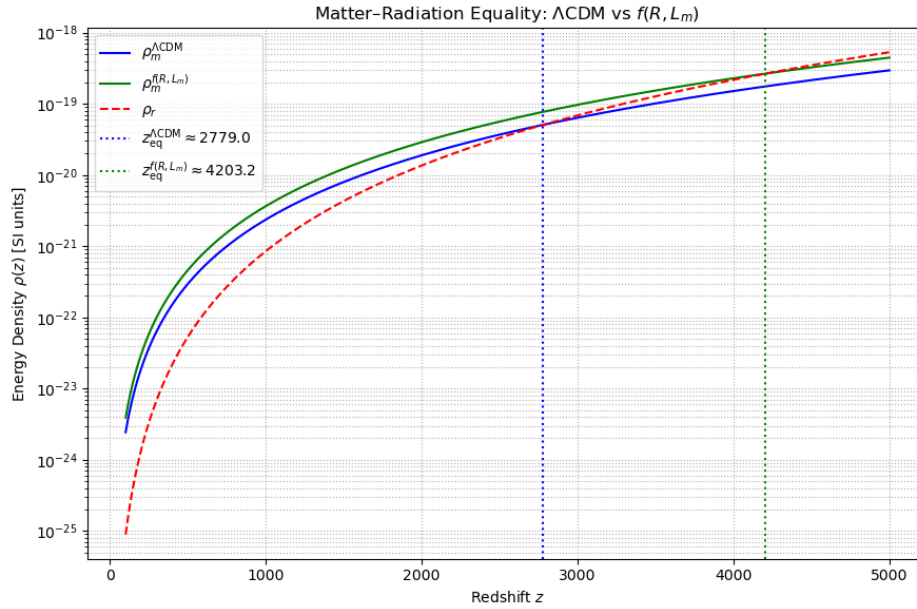


FIG. 3: Evolution of matter and radiation energy densities in both ΛCDM and $f(R, L_m)$ models. Solid curves represent matter densities—blue for ΛCDM and green for $f(R, L_m)$. The dashed red curve shows radiation. Vertical lines indicate the matter–radiation equality redshifts. The earlier equality in $f(R, L_m)$ facilitates early structure formation.

VI. CONCLUSION

In this work, we have explored the cosmological viability of the modified gravity model

$$f(R, L_m) = \alpha R + L_m^\beta + \gamma,$$

which incorporates a non-minimal coupling between curvature and matter. Through a combination of observational datasets and theoretical modeling, we constrained the model parameters using distance modulus data via chi-square minimization, Bayesian MCMC analysis, and neural network-based regression. The best-fit results indicate that the $f(R, L_m)$ framework supports a relatively high Hubble constant, $H_0 = 73.75 \pm 0.16 \text{ km s}^{-1} \text{ Mpc}^{-1}$, in close agreement with local measurements—thus offering a potential resolution to the Hubble tension.

We further investigated early-universe signatures arising from this modified gravity framework. The redshift of matter–radiation equality in $f(R, L_m)$ gravity is found to be $z_{\text{eq}}^{f(R, L_m)} \approx 4203$, significantly earlier than in the ΛCDM model ($z_{\text{eq}}^{\Lambda\text{CDM}} \approx 2779$). Moreover, the onset of nonlinear structure formation occurs at a much higher redshift, $z_c^{f(R, L_m)} \approx 25.56$, whereas ΛCDM fails to reach the standard collapse threshold ($\delta = 1.686$) by the present epoch. These findings highlight the role of the enhanced effective gravitational coupling in $f(R, L_m)$ gravity, which accelerates the growth of perturbations and may facilitate the formation of high-redshift galaxies and clusters.

In addition, we analyzed the recombination epoch via the visibility function. Both models accurately reproduce the observed recombination redshift ($z_{\text{rec}} \approx 1092.6$), but the $f(R, L_m)$ model yields a slightly broader full width at half maximum (FWHM), indicating a more extended photon decoupling duration. This subtle deviation may leave observable imprints in the CMB power spectrum.

Overall, the $f(R, L_m)$ gravity model retains consistency with key cosmological observations such as the CMB recombination epoch while offering distinct early-time predictions—namely, earlier matter–radiation equality, rapid structure formation, and extended recombination duration. These theoretical features can be probed with upcoming high-redshift galaxy surveys and 21 cm cosmology. Hence, $f(R, L_m)$ gravity stands as a compelling alternative to the ΛCDM paradigm, capable of addressing both late-time cosmic acceleration and early-universe phenomena within a unified framework.

VII. FUTURE OUTLOOK

The findings presented in this work open up several avenues for further investigation and observational testing of the $f(R, L_m)$ gravity model. Given its success in addressing both early- and late-time cosmological phenomena, this framework warrants closer scrutiny through high-precision astrophysical probes and numerical simulations.

1. High-Redshift Structure Formation

The early onset of nonlinear structure formation predicted by the model ($z_c \approx 25.56$) could be validated by upcoming observations targeting the first generation of galaxies and protoclusters. Telescopes such as the *James Webb Space Telescope* (JWST), the *Nancy Grace Roman Space Telescope*, and the *Euclid* mission

are expected to provide high-resolution imaging and redshift data for galaxies at $z > 10$, allowing direct comparison with the predicted early collapse scenarios.

2. 21 cm Cosmology and Reionization History

The timing and efficiency of early structure formation influence the reionization epoch and the 21 cm neutral hydrogen signal. Experiments such as the *Square Kilometre Array* (SKA), the *Hydrogen Epoch of Reionization Array* (HERA), and the *LOFAR* survey will be crucial in tracing the imprint of modified gravity on the cosmic dawn and dark ages. The earlier matter domination in $f(R, L_m)$ gravity may result in distinct timing and amplitude of 21 cm brightness fluctuations.

3. Cosmic Microwave Background (CMB) Anisotropies

While the recombination redshift in $f(R, L_m)$ gravity aligns with Planck 2018 results, the extended duration of decoupling could leave observable signatures in the damping tail and acoustic peak structure of the CMB power spectrum. Future CMB experiments such as *CMB-S4* and *LiteBIRD* can offer enhanced sensitivity to these subtle features and test the extended visibility function predicted by the model.

4. Large-Scale Structure and Weak Lensing Surveys

Next-generation surveys such as *LSST* (Vera C. Rubin Observatory) and *DESI* will map the distribution of galaxies and matter on cosmological scales. These datasets will enable precise reconstruction of the growth rate of structure, gravitational slip, and effective gravitational coupling $G_{\text{eff}}(z)$, providing direct tests of the dynamical predictions of $f(R, L_m)$ gravity.

5. Theoretical Developments

Further theoretical refinement is necessary to explore consistency with local gravity constraints, cosmic chronometers, and quantum stability of the model. Developing a perturbative formalism in the Newtonian gauge or performing N-body simulations under the $f(R, L_m)$ framework can yield deeper insights into small-scale structure formation and the nonlinear regime.

In summary, the distinct early-universe signatures and flexible cosmological behavior of the $f(R, L_m)$ gravity model make it an exciting candidate for next-generation cosmological investigations. The synergy between theory and precision data from upcoming missions will be essential in confirming or refuting the viability of such non-minimally coupled modified gravity theories.

ACKNOWLEDGMENTS

One of the authors (G. K. Goswami) gratefully acknowledges the facilities and stimulating research environment provided by the Inter-University Centre for Astronomy and Astrophysics (IUCAA), Pune, during

his research visits. The support and academic atmosphere at IUCAA were instrumental in shaping the progress of this work.

-
- [1] N. Aghanim *et al.* [Planck Collaboration], “Planck 2018 results. VI. Cosmological parameters,” *Astron. Astrophys.* **641**, A6 (2020), [arXiv:1807.06209](#).
 - [2] D. J. Eisenstein *et al.*, “Detection of the Baryon Acoustic Peak in the Large-Scale Correlation Function of SDSS Luminous Red Galaxies,” *Astrophys. J.* **633**, 560 (2005), [astro-ph/0501171](#).
 - [3] B. A. Reid *et al.*, “Cosmological constraints from the clustering of the Sloan Digital Sky Survey DR7 luminous red galaxies,” *Mon. Not. R. Astron. Soc.* **404**, 60–85 (2010), [arXiv:0907.1659](#).
 - [4] “GALEX–SDSS Catalog for Statistical Studies”, Tamás Budavári *et al.* *ApJ* 694 1281(2009)
 - [5] A. G. Riess *et al.*, “Observational evidence from supernovae for an accelerating universe and a cosmological constant,” *Astron. J.* **116**, 1009 (1998), [astro-ph/9805201](#).
 - [6] S. Perlmutter *et al.*, “Measurements of Ω and Λ from 42 high-redshift supernovae,” *Astrophys. J.* **517**, 565 (1999), [astro-ph/9812133](#).
 - [7] D. H. Weinberg *et al.*, “Observational probes of cosmic acceleration,” *Phys. Rept.* **530**, 87–255 (2013), [arXiv:1201.2434](#).
 - [8] T. P. Sotiriou and V. Faraoni, “ $f(R)$ theories of gravity,” *Rev. Mod. Phys.* **82**, 451–497 (2010), [arXiv:0805.1726](#).
 - [9] H. Shabani and M. Farhoudi, “ $f(R, T)$ cosmological models in phase space,” *Phys. Rev. D* **88**, 044048 (2013), [arXiv:1306.3164](#).
 - [10] Y. Fujii and K. Maeda, *The Scalar-Tensor Theory of Gravitation*, Cambridge University Press, Cambridge, UK (2003).
 - [11] S. Nojiri and S. D. Odintsov, “Unified cosmic history in modified gravity: From $f(R)$ theory to Lorentz non-invariant models,” *Phys. Rept.* **505**, 59–144 (2011), [arXiv:1011.0544](#).
 - [12] T. Harko and F. S. N. Lobo, “ $f(R, L_m)$ gravity,” *Eur. Phys. J. C* **70**, 373 (2010), [arXiv:1008.4193](#).
 - [13] R. Myrzakulov, “Reconstruction of $f(R, L_m)$ gravity: Expansion history and observational constraints,” *Eur. Phys. J. C* **72**, 2203 (2012), [arXiv:1207.1039](#).
 - [14] G. K. Goswami and J. P. Saini, “Growth Rate Analysis in $f(R, L_m)$ Gravity: A Comparative Study with Λ CDM Cosmology,” [arXiv:2507.04079 \[gr-qc\]](#) (2025).
 - [15] P. J. E. Peebles, “Recombination of the Primeval Plasma,” *Astrophys. J.* **153**, 1 (1968).
 - [16] Ya. B. Zel’dovich, V. G. Kurt, and R. A. Sunyaev, “Recombination of Hydrogen in the Hot Model of the Universe,” *Sov. Phys. JETP* **28**, 146 (1969).
 - [17] S. Seager, D. D. Sasselov, and D. Scott, “A new calculation of the recombination epoch,” *Astrophys. J. Lett.* **523**, L1 (1999), [arXiv:astro-ph/9909275](#).
 - [18] S. Bashinsky and U. Seljak, “Signatures of Relativistic Neutrinos in CMB Anisotropy and Matter Clustering” *Phys. Rev. D* **69**, 083002 (2004), [arXiv:astro-ph/0310198](#). <https://arxiv.org/abs/2507.04079>
 - [19] W. Hu and N. Sugiyama, “Toward understanding CMB anisotropies and their implications,” *Phys. Rev. D* **51**, 2599 (1995), [arXiv:astro-ph/9411008](#).
 - [20] T. M. C. Abbott *et al.* [DES Collaboration], “Dark Energy Survey Year 3 results: Cosmological constraints from galaxy clustering and weak lensing,” *Phys. Rev. D* **105**, 023520 (2022), [arXiv:2105.13549](#).
 - [21] Z. Safari, K. Rezazadeh, and B. Malekolkalami, “Structure formation in dark matter particle production cosmology,” *Phys. Dark Universe*, **37**, 101092(2022)
 - [22] J. E. Gunn and J. R. Gott, “On the Infall of Matter Into Clusters of Galaxies and Some Effects on Their Evolution,” *Astrophys. J.* **176**, 1 (1972).

- [23] Edward Kolb, *The Early Universe*, CRC Press, Boca Raton(1990)
- [24] V. Mukhanov, *Physical Foundations of Cosmology*, Cambridge University Press, Cambridge (2005).
- [25] S. Weinberg, *Cosmology*, Oxford University Press, Oxford (2008).